Performance improvement of an industrial Stirling engine heat pump

Ron Zevenhoven [a], Umara Khan [b], Carl Haikarainen [c], Loay Saeed [d], Tor-Martin Tveit [e], and Henrik Saxén [f]

[a] *Åbo Akademi University, Turku, Finland, ron.zevenhoven@abo.fi,* ***CA***
[b] *Åbo Akademi University, Turku, Finland, umara.khan@abo.fi*
[c] *Åbo Akademi University, Turku, Finland, carl.haikarainen@abo.fi*
[d] *Åbo Akademi University, Turku, Finland, loay.saeed@abo.fi*
[e] *Olvondo Technology, Holmestrand, Norway, tor-martin.tveit@olvondotech.no*
[f] *Åbo Akademi University, Turku, Finland, henrik.saxen@abo.fi*

Abstract:
After widespread use for refrigeration and cooling, heat pumps (HPs) are also becoming mainstream for private and public building heating. Driving forces are the need to reduce greenhouse gas emissions and the increased availability of renewable electricity. Nowadays, HPs find use in industry, choosing for low temperature (waste) heat and cheap (renewable) electricity rather than a combustion system for the production of process heat. However, temperatures above 150°C still present challenges for HP systems based on a vapour-compression process, being limited by compressor technology and availability of suitable refrigerants. So-called very high temperature heat pumps (VHTHPs) based on alternative processes using renewable electricity are an attractive "green" route to producing ~200 °C steam. This paper describes work aiming at improving the performance, reliability and efficiency of an industrial Stirling engine-based heat pump system in operation at a pharmaceutical research facility. It is funded by the EU Horizon 2020 FTI programme, targeting reduced greenhouse gas emissions, efficient use of energy and increased use of renewable energy resources. In short, heat output shall increase from 500 kW to 750 kW closer to 200°C rather than 180°C with input heat of ~ 30°C while efficiency expressed as coefficient of performance (COP_{HP}) increases from 1.4 – 1.5 to 1.8 –1.9. The approach is to increase the pressure of the (helium) medium, while changes to the hardware would involve new designs for the internal heat exchanger, regenerator, piston rod seal, piston rings and other seals. CFD and structural mechanics models were used to simulate existing and future designs for heat exchangers, regenerator and seals while process dynamics simulations showed the response to, for example, small leaks and the effect of dissimilar temperature gradients in the heat exchangers or regenerator porosity. The results show how the existing system could be improved to obtain the enhanced performance aimed at.

Keywords:
Heat pump system, Stirling engine, increased output, efficiency, system dynamics

1. Introduction

The first decades of the 21st century have shown transitions and changes towards energy systems that have a higher efficiency, lower or zero emissions of greenhouse gases and a smaller environmental footprint in general. In today's world, the increased availability of electricity from renewable sources may on one hand be intermittent but on the other hand is more predictable than the pricing levels for natural gas. Heat pumps (HPs) have a long history with consumer products for refrigeration and air conditioning and can in principle use a cheap renewable source for both input heat and electricity. System purchases by users are nonetheless often motivated by an attractive coefficient of performance (COP). Industry is increasingly implementing HP technology that circumvents the formation of CO_2 when producing heat, although reaching sufficiently high temperatures > 150°C may be challenging (being limited by compressor technology and availability of suitable refrigerants). So-called very high temperature heat pumps (VHTHPs) [1] based on alternative processes using renewable electricity are an attractive "green" route to ~200 °C steam.

A Stirling engine-based heat pump is one approach towards higher output temperatures. The so-called HighLift concept based on this [2] is applied in the milk and dairy products industry and, for the work

presented here at AstraZeneca's R&D centre in Gothenburg Sweden where three units each produce 500 kWth of 1 MPa steam. Figure 1 shows two of the three current heat pumps. More detail on recent and current performance of the HPs at AstraZeneca is given elsewhere [3]. This paper reports on several critical design and performance assessments and suggestions for design of the larger HPs, with respect to output and efficiency on one hand and system reliability on the other.

Figure 1. Two of the three heat pumps currently installed at AstraZeneca's R&D facility in Gothenburg, Sweden. Heat is transferred to the heat pump from the heat recovery circuit and steam is delivered from the heat pumps' steam generators to the steam distribution system. The third heat pump is installed on the opposite side of the room.

The approach followed for this was to

1. identify and reduce losses of efficiency, i.e. energy conversion that does not benefit the heat output of the engine, and
2. apply multi-objective optimization to find optimum design and operation parameters and set points for apparently conflicting goals.

For 1) computational fluid dynamics (CFD) and heat transfer calculations were made using ANSYS Fluent (v 19.2) while for 2) a commercial modelling tool SAGE is used, in combination with modelling using Simulink. In order to improve reliability the focus was on the seals that separate the different media (water, helium, lubrication oil, air) from each other and from the surroundings. By using improved designs for rate-limiting components, the servicing interval of HighLift HPs shall increase from the current 4000 h to approximately 8000 h. Structural mechanics simulations using COMSOL (v 5.4) were used to calculate forces and deformations on seal rings for different dynamic operational situations, including future modes of operation that would give better energy efficiency. Clearly, the objectives are strongly intertwined and therefore were conducted in parallel.

2. Optimisation of heat pump efficiency

2.1. Theoretical considerations

A challenge related to the goals of increasing output as well as efficiency, viz. the HighLift concept and its development, is that it conflicts with the thermodynamics that describes heat engines if the goals are simplified to having

- a higher temperature at the hot (water) side of the engine and a larger flow of heat carrier (helium) which can be achieved by raising the pressure of operation, and
- a higher coefficient of performance (COP_h), defined as heat output Q_{out} obtained per input of work (here electricity) W, with energy balance $Q_{out} = W + Q_{in}$, and $COP_h = Q_{out}/W$.

For an ideal, reversible (rev) heat engine the highest theoretical (Carnot) efficiency is defined as

$$COP_{\text{Carnot}} = \frac{Q_{\text{out,rev}}}{W} = \frac{Q_{\text{out,rev}}}{Q_{\text{out,rev}} - Q_{\text{in,rev}}} = \frac{T_{\text{H}}}{T_{\text{H}} - T_{\text{L}}} = \frac{1}{1 - \frac{T_{\text{L}}}{T_{\text{H}}}} \qquad (1)$$

with higher and lower temperatures of operation T_{H} and T_{L} (expressed in K). This shows that raising the output heat temperature T_{H} with fixed T_{L} will inevitably result in a lower efficiency, or COP_h. For an engine that heats water from $T_{\text{L}} \sim 300$ K to $T_{\text{H}} \sim 450$ K the theoretical maximum coefficient is $COP_{\text{Carnot}} \approx 3$. Current operation of the HighLift Stirling HP (500 kW per engine, heating water to 180°C) gives $COP_h = 1.4 – 1.5$: the goal is to raise it to $COP_h = 1.8 – 1.9$, while heating water with an output of 750 kW. A main means of achieving this is a system charge pressure elevation from 5 MPa (average) to 7.5 MPa (average).

A more general approach of efficiency improvement of real systems involves suppressing irreversibilities that arise from:

- friction between moving parts
- heat transfer across large temperature differences
- viscous flow friction in fluid flow lines and flow inlet/outlet section
- compression and expansion losses
- material losses as a result of leakage

Reducing friction between moving parts can be achieved by proper design of rigid and flexible parts, and lubricant oils. Heat transfer is impossible without a temperature difference and a trade-off must be made (based on costs) between a large area for heat exchange operating with small temperature difference or vice versa: the first option gives higher losses. Viscous flow losses can be directly related to pressure drop and obviously a leakage of material at elevated pressure and temperature implies an obvious loss of energy. The first three items listed will result in a production of entropy at a rate $\dot{S}_{\text{gen}}$ which can be used to quantify losses as $\dot{W}_{\text{loss}} = T^{\circ} \cdot \dot{S}_{\text{gen}}$ (J/s, Watt). Here, T° is the temperature of the surroundings, in K (say, 288 K). Fortunately, viscous flow friction results in heat that is taken up by a flow that is to be heated, which is not at all a full loss for a Stirling engine heat pump. For heat Q at temperature T produced from work W, the losses equate to $W \cdot (T^{\circ}/T)$. A larger electricity input is needed in order to cover for these losses. See also Bejan (1997) [4] or Szargut et al. (1989) [5].

With an electrical-to-mechanical energy conversion efficiency η_{elec} and heat losses $\dot{Q}_{\text{loss}}$ to the surroundings equation (1) can be reworked to

$$COP_h = \frac{\dot{Q}_{\text{out}}}{\dot{W}_{\text{in}}} = \frac{\dot{Q}_{\text{in}} - \dot{Q}_{\text{loss}} + \dot{W}_{\text{in}} - \dot{W}_{\text{loss}} + \dot{W}_{\text{loss giving heat}}}{P \cdot \eta_{\text{elec}}} < \frac{\dot{Q}_{\text{out,rev}}}{\dot{W}_{\text{rev}}} \qquad (2)$$

correcting for input energy not contributing to raising the temperature of the water. Currently electric power input $P \sim 315$ kW with $\eta_{\text{elec}} \sim 95\%$, $\dot{Q}_{\text{loss}} \sim 30$ kW and $\dot{Q}_{\text{in}} \sim 300$ kW. The assessment for the heat exchange applies to the regenerator as well, while a further source of losses are those related to real compression and expansion vs. ideal processes – see [5, p. 119].

Combining all this gives with current operation with 300 kW effective power input that 45-50 kW of this is lost via entropy losses in the heat exchangers, while 55- 65 kW is lost in the regenerator plus ~ 40 kW compression/expansion losses. These add up to ~ 45% of the effective electricity input which, using the expressions for COP_h with heat input $\dot{Q}_{\text{in}}$ being of the order of 300 kW explains the value $COP_h = 1.4 – 1.5$; more details are given in [3].

For the heat exchangers, a different design that gives small temperature gradients would be beneficial while for the regenerator the reduction of viscous flow losses is most beneficial.

2.2. Improvements to the heat exchanger + regenerator

For the heat exchangers, optimisation variables are the number of tubes, the inner diameter of the tube, wall thickness, tube length, tube material and pitch. The total length of the heat exchangers and regenerator are constraints. Optimising (in a coordinated manner) the heat exchangers, shaft speed and/or phase angle shall increase the efficiency of the system. (Reducing heat losses through well-designed insulation will also increase efficiency, especially at high temperature; this will also lower noise levels.) Changes to heat regenerator diameter and the spacing of the tubes (preserving minimal dead-space between shell and tube heat exchangers) will be tested. Presumably the regenerator packing density (test range 0.7-0.9) needs to be modified.

CFD simulations using ANSYS Fluent (v 19.2) were made on the double heat exchanger + regenerator assembly. The computational grid for the imported geometry was created with the use of ANSYS grid generator as shown in Figure 2.1. A grid (in)dependence analysis was conducted before the simulation setup. The first step of meshing was defining global mesh setting (physics, meshing method, contact and connection points' generation). After that, the local mesh setting was inserted where quality, sizing, and assembly making properties were defined. Finally, the surface mesh and inflation were previewed, and the mesh was generated. Hexahedral cells were generated in the different volume spaces of the heat exchangers (hot heat exchanger, regenerator, cold heat exchanger and elbow and cup for the inlets), so that the grid can be transformed by the method of layering in each time step. The quality of mesh was assessed by mesh metric and chart (skewness and orthogonal quality).

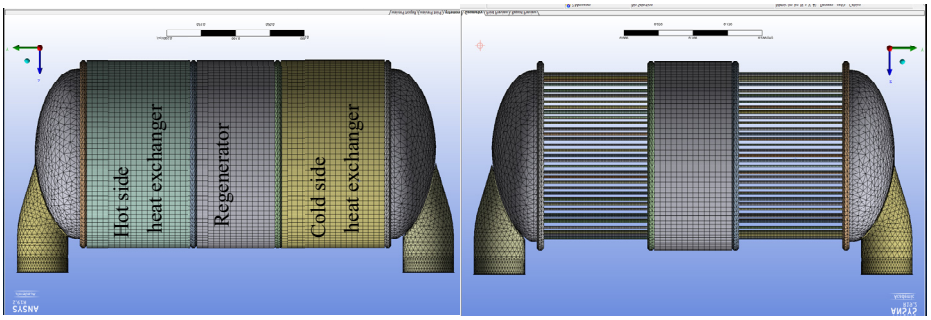

Figure 2. Generated mesh of heat exchangers and regenerator

The ANSYS Fluent double precision solver was used, along with a pressure-based coupling algorithm. The regenerator was modelled as a porous medium. The thickness of all the walls was set equal to zero since these would not give a heat transfer resistance while adding much complication to the calculation mesh. The working fluid of the engine is helium. In the simulations, the equation of state of the ideal gas was applied. Viscosity is defined by kinetic theory, while the thermal conductivity is temperature dependent. All the solid parts of the engine are made of stainless steel. For density and heat capacity, the kinetic theory equation from the software was used.

Heat is absorbed and rejected via the heater and cooler, respectively. Ideally, the temperatures of the heater and cooler are constant. Consequently, convection between working gas and the inner wall of the respective heat exchanger was applied. The inlets were selected to be mass flow inlets and while the outlet is a pressure outlet. A UDF was linked to the model for defining the time-dependent periodic boundary conditions, programmed in C.

With the helium medium flow changing direction about ten times per second, entering the heat exchangers average at 500 K (227°C), the temperatures of the water flowing outside the helium-containing tubes is taken constant at 180°C and 40 °C for the hot and cold sides, respectively.

Findings correlate with reporting by others [6,7]: heat exchange gives losses resulting from the temperature differences while the regenerator gives most losses as a result of viscous flow friction. Examples of calculated results are given in Figures 3 - 5, showing velocity intensity and temperature profiles.

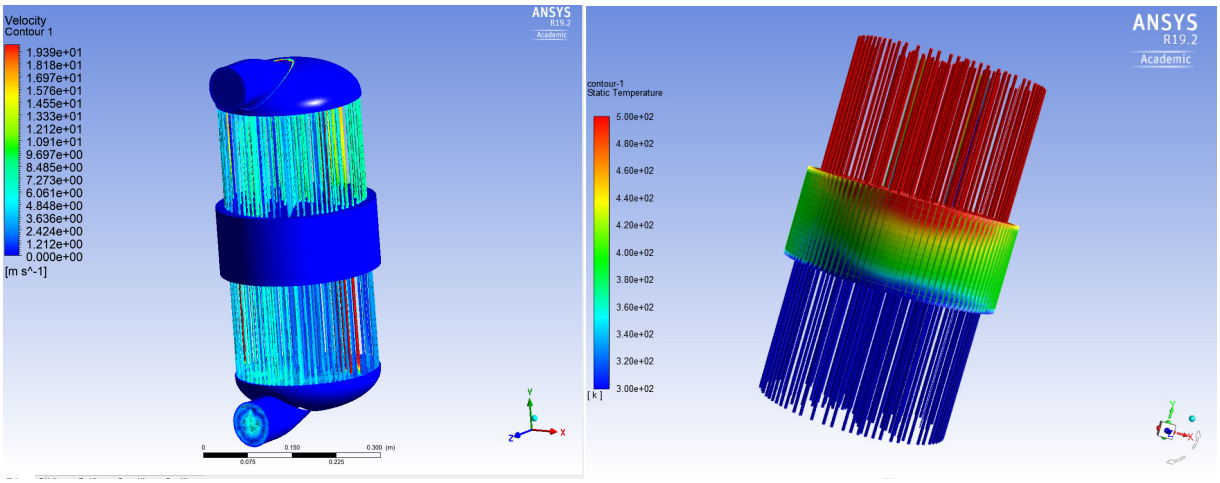

Figure 3. CFD simulated results for (cycle averaged) pressure (~5 MPa) velocity (0 – 20 m/s) (left) and temperature (300-500K) (right) for 500 kW heat output operation

The velocity profile can be divided into various segments. In the first segment, helium gas, which is flowing in the elbow and cup inlet with an average velocity of 2-5 m/s, starts to accelerate as it moves through the hot heat exchanger tubes. The velocity profile of the gas inside the regenerator is not uniform. The cross-sectional area changes rapidly at the connections between heat exchanger tubes and the regenerator. The regenerator shows three prominent velocity profile sections. The first section is the interface where the gas exits the hot heat exchanger tubes and enters the regenerator. There is a sudden drop in the gas velocity at that section. Inside the regenerator, the velocity will be higher in the porous structure than in other non-porous parts of it. Because of this accelerated velocity, a pressure gradient occurs within the regenerator.The third section is the end where gas exits the regenerator and enters the cold heat exchanger tubes. In this section, velocity starts to increase to approximately average 10 m/s. The velocity change is more significant in case of hot heat exchanger tubes. Pressure drop arises for a number of reasons such as viscous friction, design of heat exchangers and the joints where a sudden change in cross-section area or velocity of the gas occurs.

The CFD simulation results (Figure 3) show a non-uniform distribution of gas temperature in the heat exchangers and regenerator, which strongly affects the heat transfer coefficient. In the heat exchanger tubes, the temperature of the gas is higher than that of the water surrounding it. Due to this slight temperature difference, some of the heat is rejected in the hot heat exchanger toward the heater walls. The temperature of the gas in the cold side of the regenerator is around 340 K while gas temperature near the hot side of regenerator is about 500 K.

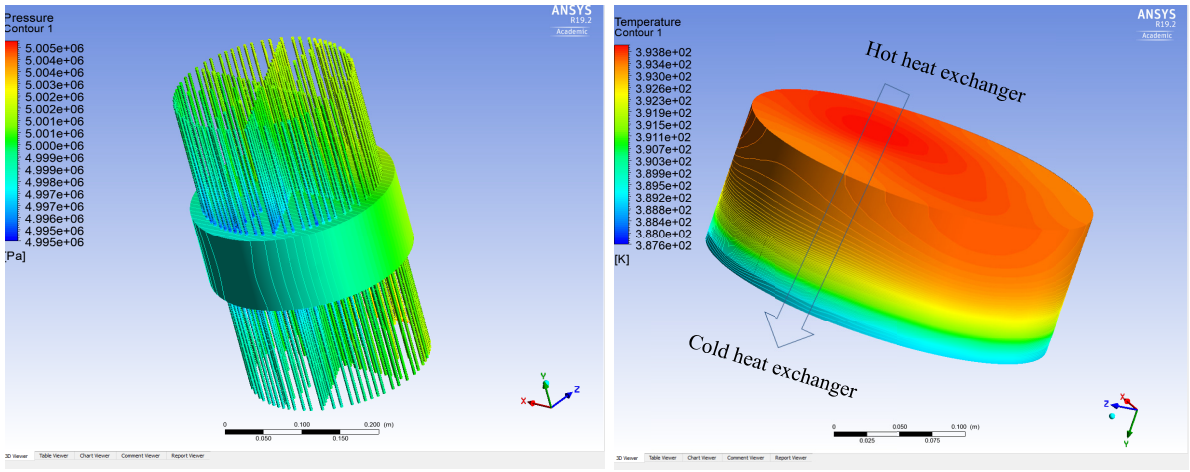

Figure 4. CFD simulated results for (cycle averaged) pressure (~5 MPa) (left) and cross-section of temperature of regenerator (387-393 K) (right) for 500 kW heat output operation

Pressure contours from the CFD simulation (Figure 4, left) shows pressure gradients in the hot heat exchanger, cold heat exchanger and regenerator when a steady cycle is achieved. Despite its good heat transfer properties, the porous structure of the regenerator also blocks some of the gas flowing in the heat exchangers and causes a pressure drop. This can be seen from the variation of pressure in the figure. In the case with 10 Hz operating frequency, the average pressure drop in the regenerator is about 10 kPa. In general, the pressure drop inside the heat exchanger tubes and regenerator are negligible compared to the pressure drop in compression and expansion spaces of the Stirling engine. The temperature profile inside the regenerator is given as well (Figure 4, right)

Results for the original design of elbow and cup inlet/outlet show that the bend in the elbow creates turbulence, which causes restricted flow at the inclined point of contact. This could result in avoidable heat losses. Comparing it with another geometrical design shows that a straight-line inlet for the gas into the heat exchangers would be preferable over the current curved elbow inlet since it gives a lower pressure drop. Pressure and velocity distribution are non-uniform inside the regenerator (Figure 5).

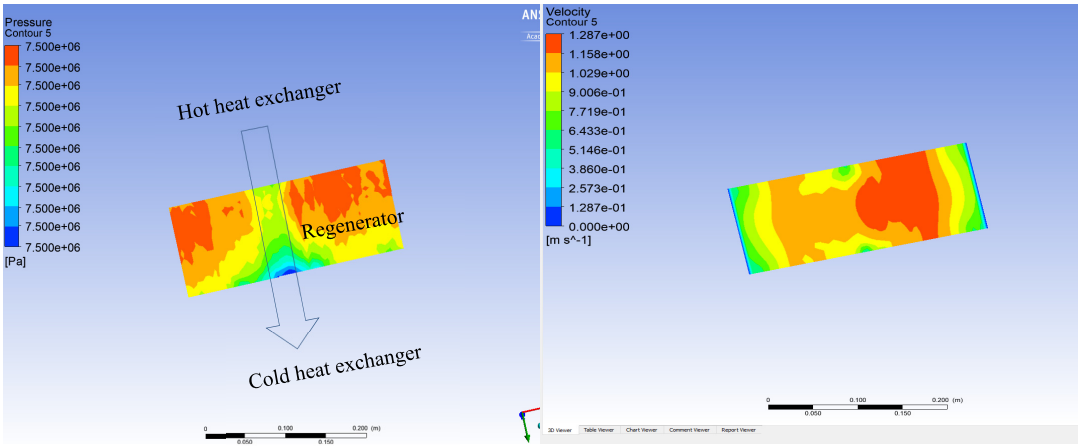

Figure 5. CFD simulated results for regenerator (cycle averaged) cross-section for pressure (~7.5 MPa) (left) and velocity (0 – 13 m/s) (right) for 750 kW heat output operation

The regenerator porosity was varied from 0.6 to 0.9 at a constant water temperature of 180 °C for the hot heat exchanger and water temperature of 28 °C in the cold heat exchanger, and the effects on the heat exchanger performance are analyzed. In both cases, it is observed that if regenerator porosity is increased from 0.6 to 0.8, it leads to higher regenerator effectiveness as well as higher heat transfer. When the porosity is increased further to 0.9, more heat is lost to the surroundings as the decrease in hydraulic resistance of the non-uniform flow inside the heater tubes affects the overall heat transfer. Thus, an overall porosity of between 0.78-0.83 seems optimal considering the gas flow.

The diameter of the wires that are wound and packed to form the regenerator packing material was found important. The results showed that by reducing the diameter for the same mass flow rate of gas, there is an increase in gas velocity in the heat exchangers and the regenerator resulting in an increase in the heat transfer by 25-35%. The heat losses for such cases are reduced.

The effects of increased cycling frequency (10.0 → 12.5 Hz), and/or increased pressure (5 ±1.3 MPa → 7.5 ± 1.5 MPa) were found to be beneficial, improving the heat transfer while not affecting pressure drop very much. Altogether, the findings on the effects of operational and design parameters follow very well the trends and findings reported in the (scarce) open and relevant literature, such as [6,7].

2.3. Improvements to the system based on system performance simulation

Simulation and optimization of the Stirling engine heat pump using Sage software [8] shows that improvement in both efficiency and output ought to be possible by changing design parameters of the heat exchangers and the regenerator. Modelling the heat pump system consisting of double acting piston-cylinders, heat exchangers and regenerators, the optimization could be carried out for the system as a whole, with the system performance evaluated through the coefficient of performance (COP_h) and the heat output ($\dot{Q}_{out}$). Considered optimization variables were heat exchanger lengths, tube diameters and number of tubes, as well as regenerator porosities and wire diameters. Additionally, optimization was performed at different average system pressure levels up to 7.5 MPa, and with system frequencies between 7 and 12.5 Hz.

Figure 6 shows Pareto fronts of maximizing COP_h and $\dot{Q}_{out}$ at a 5 MPa pressure level and 12.5 Hz system frequency, given different optimization constraints. As can be seen in Figure 6, the best results were reached when optimizing the system without restrictions on component lengths and treating hot-side heat exchangers (coolers) and cold-side heat exchangers (heaters) separately. However, differences between results with separate designs for heaters and coolers versus results with equal heaters and coolers are very small. Changes common to both heaters and coolers combined with changes in the regenerator can thus be said to give the biggest performance improvements. Since performance close to optimal can be reached with equal parameters for coolers and heaters, such a design could for the sake of simplicity be recommended.

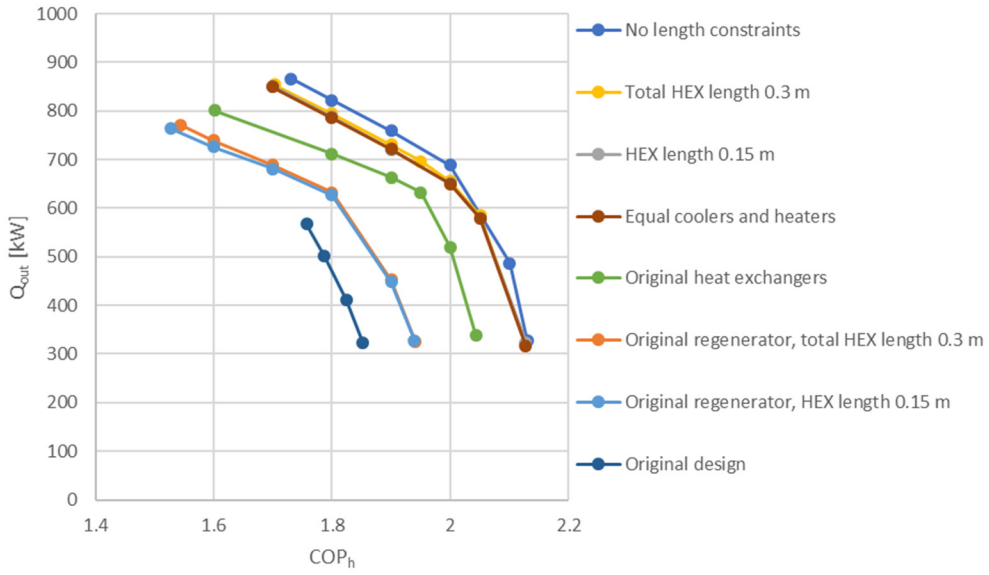

Figure 6. Optimal Pareto fronts balancing system efficiency and heat output with different parameter constraints with 5 MPa charge pressure and 12.5 Hz frequency

The optimizations suggested increasing the number of heat exchanger tubes and decreasing their diameters. For instance, a design optimized at a 5 MPa pressure level, favouring high efficiency, could have heat exchangers featuring 2200 tubes with diameters 2.0 mm, and regenerators with porosities 0.89 and wire diameters 50 µm. The simulations indicate that this type of a design could increase efficiency and additionally work well at 7.5 MPa pressure levels. However, optimal design of a specific system would additionally depend on desired operating temperatures and restrictions regarding component manufacturing.

3. Increase of heat pump reliability

3.1. Improvements to the system based on system performance simulation

A model of the Stirling heat pump system was developed using Simulink software in order to study phenomena occurring in the system. In particular, the issue of emerging pressure imbalances, i.e., fluctuating pressure differences between the top and bottom circuits, was studied. Simulations incorporating different types of gas leakage between the circuits was performed. It was found that a leakage model imitating so-called pressure reversal leakage in the pistons (i.e. leakage occurring in the piston rings at the point of the system cycle when the pressures shift from higher in the top circuit to higher in the bottom circuit and vice versa) could display similar pressure behaviour as the real system.

The leakage was modelled as a valve opening whenever the pressure difference between the circuits was sufficiently small, allowing for a small gas flow between the circuits, in both directions. The pressure imbalance then emerges depending on the system pressure level and frequency, and changes in the size of the leakage and the time when these changes take place. Figure 7 presents an example of the behaviour of measured pressure (top figure) and the computational counterpart (bottom figure) simulated by making small changes in the valve opening at time instants corresponding to pressure changes in the measured data.

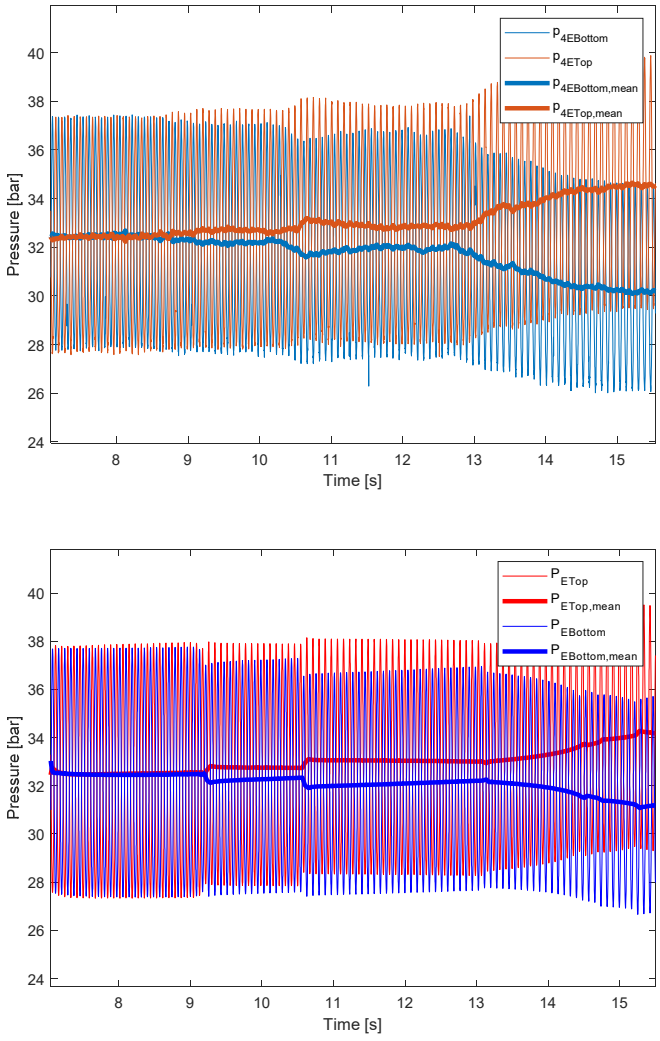

Figure 7. Measured data featuring increasing pressure differences between top and bottom circuits (top figure) mimicked with the simulation model by applying small changes in piston gas leakage (bottom figure)

Starting at a mean pressure level of 3.25 MPa, the pressure in the top circuit is gradually increasing, while the pressure in the bottom circuit is decreasing correspondingly. With the leakage modelled as a gap around the piston, the changes in the gap size giving rise to the pressure behaviour in Figure 7 are of the order 0.1 mm, indicating that the balance between the systems can be quite sensitive in these conditions.

It is interesting to note that such pressure differences can appear when gas flow through the leakage is allowed in both directions, with a mathematical model following quite a simple logic. It was also found that both increases and reductions in the valve opening can lead to increased pressure differences, indicating complex behaviour already with a simple model. Simulations showed that built-in bypass gas paths to prevent pressure imbalances would have to be so large that system efficiency would be affected negatively. Improved piston rings might solve the problem, but without detailed knowledge of where and how the assumed gas leakage happens, it is difficult to say what type of piston ring would be required to prevent it.

3.2. Piston rod seal design and performance

The study also involved dynamic modelling of the forces and stresses on the pumping Leningrader (PL) seal of piston rod using COMSOL Multiphysics software (v 5.4). Historically, pumping Leningrader (PL) seals were successfully used as rod seals for automotive Stirling engine applications [9]. The main purpose of the PL seal is to prevent the leakage of high-pressure gas (mainly helium) from the Stirling engine. Also, it should avoid oil migration to the piston rings area which can cause a serious problems. For example, oil migration can increase the wear rate of the piston rings [10]. In addition, oil migration with time could lead to regenerator contamination [11] and clogging, which leads to a significant reduction in heat transfer and engine performance [12, 13]. Still, a small leakage is acceptable in most high-pressure Stirling engines using helium [10]. Sometimes, lubricant additives may form a solid deposit, which may cause wear. In addition, the additives can become very chemically active especially when the temperature reaches a certain level and may cause further wear by corrosion [14].

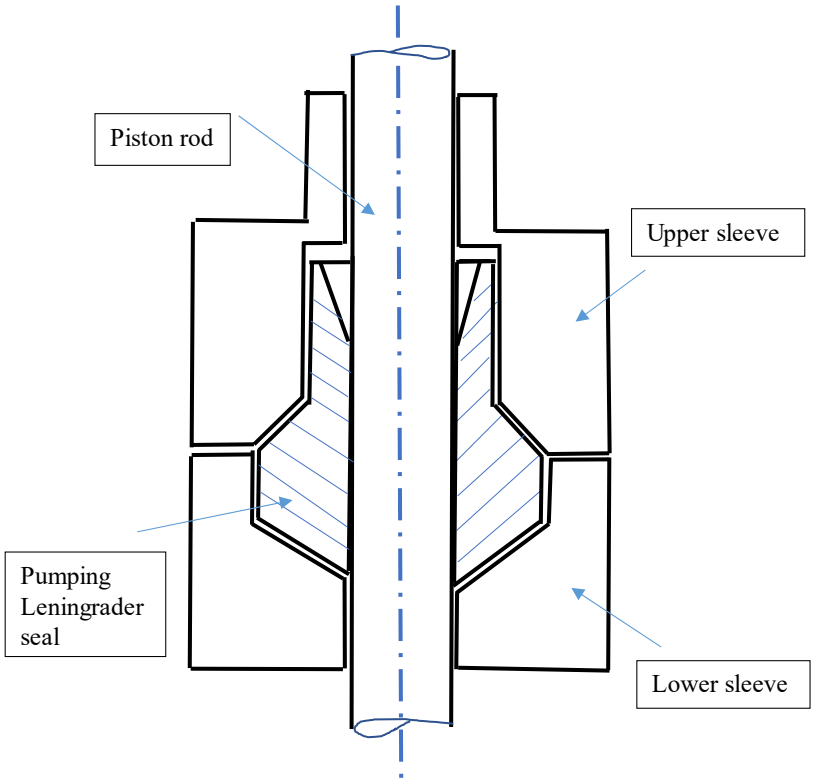

Figure 8 Schematic of the piston rod assembly (dimensions not to scale)

Figure 8 shows an enlarged detailed drawing of the seal surrounded by the sleeves on the piston connecting rod. The material of the seal is polytetrafluoroethylene (PTFE) Teflon. This is a semi-crystalline polymer widely used for its very low friction coefficient, but also for its numerous other advantages such as electrical insulation, high resistivity to corrosion and high thermal stability [15]. The PTFE type used for the seal is Fluteck P7500 CA. It is a filled compound on virgin PTFE containing 25% carbon coke for ram extrusion, compression and isostatic moulding. This product has very good properties, including improved thermal dimensional stability, improved creep resistance, improved compression strength, good cold flow reduction, exceptional temperature resistance, and excellent wear resistance, excellent resistance to abrasion, improved surface hardness, excellent chemical stability and good thermal and electrical conductivity [16].

The COMSOL simulation results show that increasing the average system pressure from 5 MPa to 7.5 MPa will have an effect on the total displacement of the seal, on the other stresses and on the oil-film pressure. Total displacement was not significant as this was increased by only 1.6 µm – see Figure 9a. Also, the normal stress and lubrication oil film pressure were increased when the total average system pressure increased while the shear stress decreased. The highest von Mises stress was 11.2 MPa (Figure 9b) and highest Tresca stress was 12.9 MPa (Figure 9c) [17]. Both latter values are smaller than the maximum tensile strength (13.9 MPa) of the PL seal material, which means that the material of the PTFE seal type should be capable of taking the highest stress during engine operation when the pressure will be increased from 5 MPa to 7.5 MPa (average pressure).

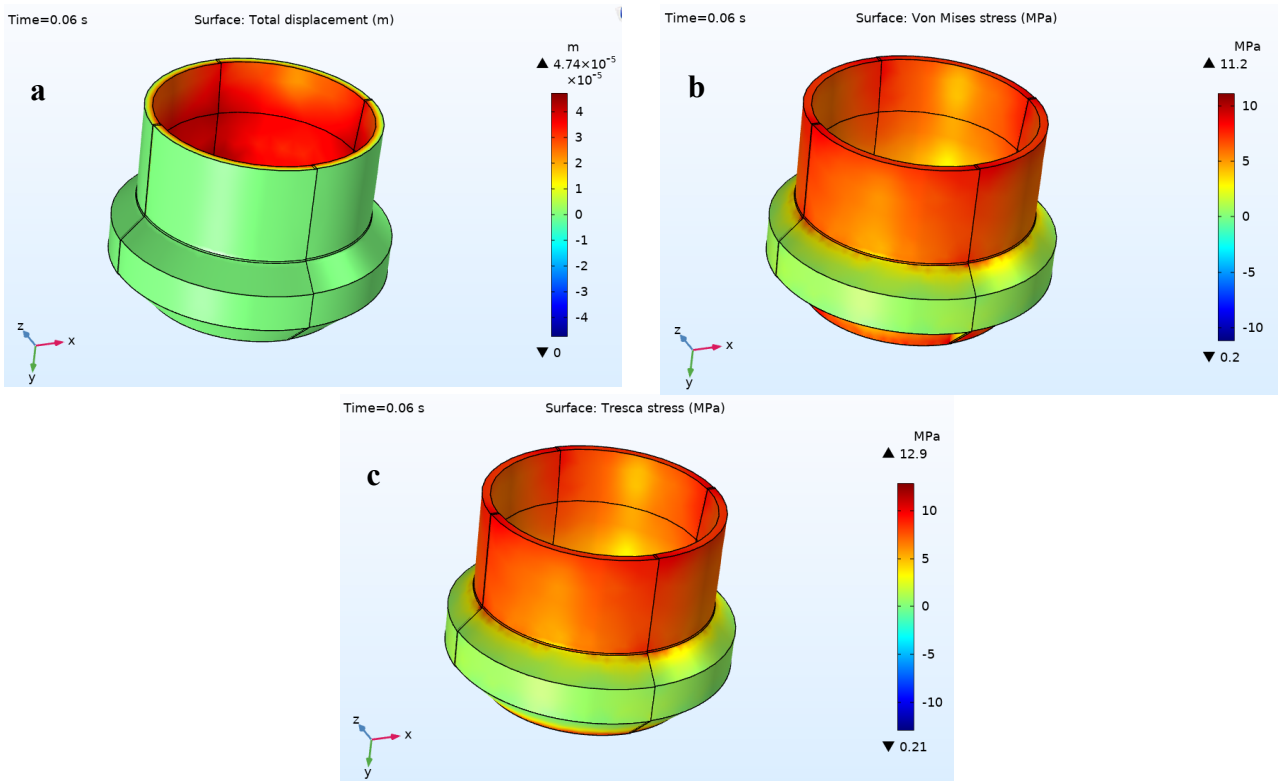

Figure 9 (a) Deformation of the seal surface (in m × 10^{-5}) at t = 0.06 s of the cycle time. (b) Calculated Von Mises stress and (c) Calculated Tresca stress

4. Conclusions

A proven concept is described for a Stirling engine operated as an industrial-scale heat pump (HP), delivering steam at 180°C at AstraZeneca's R&D facility in Gothenburg, Sweden. Current activities are described that involve improving system efficiency and reliability while increasing heat output from 500 kW to 750 kW, at the same time raising the TRL of the heat pump from level 7 to level 9.

The starting point for the change is an increase in average pressure from 5 MPa to 7.5 MPa. Heat output and energy conversion efficiencies are optimised which in theory implies two conflicting objectives. System simulation using Sage software combined with CFD calculations (ANSYS Fluent) gives design information on how to modify the heat exchangers and the regenerator. For improved reliability of the HighLift concept, simulations using Simulink show the possible impacts of HP system pressure imbalances and possible leakages while structural mechanics simulation using COMSOL allow for assessment of possible deformation or failure of the piston seal, or oil or helium leakages via this part. With no significant challenges ahead to be expected, a lot of guiding information and confidence for the next steps have been obtained, with the larger 750 kW heat pump currently under construction. A new heat exchanger and regenerator design is used as the main feature besides minor improvements and adjustments to seals and rings while many other components can stay the same. The system simulation work showed that much information on the performance dynamics of the total HP system can be obtained from the vast amount of data that is continuously collected on-line, motivating an increased emphasis on this while going from one TRL level to the next. Thus the market for this technology for the production of heat as required in industry can expand in a world where energy systems are increasingly "de-fuelled" and emissions-free.

Acknowledgements

The work described in this paper is partly financed by the European Commission under the Horizon 2020 Fast Track to Innovation programme, grant agreement number 831062 (2019-2021). The authors thank the project co-workers at Olvondo Technology and AstraZeneca for input data, technical drawings of system components and other support.

Nomenclature

CFD *Computational fluid dynamics*
COP *Coefficient of performance*
HEX *Heat exchanger*
HP *Heat pump*
P *Power, W*
PL *Pumping Leningrader*
PTFE *Polytetrafluoroethylene (Teflon)*
Q *Heat, J*
$\dot{Q}$ *Heat rate, W*
$\dot{S}$ *Entropy rate, W/K*
T *Temperature, °C or K*
TRL *Technology readiness level*
UDF *User-defined function*
VHTHP *Very high temperature heat pump*
W *Work, J*
$\dot{W}$ *Work rate (power), W*

Greek symbols

η *Efficiency, - or %*

Subscripts and superscripts

Carnot *Carnot*
elec *Electric*
gen *Generated*
h *Heat pump*
H *Higher (temperature)*
L *Lower (temperature)*

rev *Reversible*
° *Surroundings conditions*

References

[1] Arpagaus C, Bless, F, Uhlmann M, Schiffmann J, Bertsch S. High temperature heat pumps: Market overview, state of the art, research status, refrigerants, and application potentials. Energy 2018; 152: 985-1010.

[2] HighLift series SPP 4-106 Stirling cycle-based heat pump. Available on-line:
<http://www.olvondotech.no/the-technology/> [accessed 15.1.2020].

[3] Tveit, T.-M., Johansson, M.N., Zevenhoven, R. "Environmentally friendly steam generation using VHTHPs at a pharmaceutical research facility" accepted for 13th IEA Heat Pump Conference, Jeju, South Korea, September 21-24, 2020, paper no. 4

[4] Bejan, A. Advanced Engineering Thermodynamics 2nd ed., John Wiley & Sons, 1997

[5] Szargut, J., Morris, D., Steward, F.R. Exergy Analysis of Thermal, Chemical and Metallurgical Processes. Hemisphere Publishing Co, 1988.

[6] Sowale, A., Kolios, A. "Thermodynamic performance of heat exchangers in a free piston Stirling engine" Energies 11 (2018) 505 (open source) Available at: <https://www.mdpi.com/1996-1073/11/3/505 > [accessed 15.1.2020]

[7] Zarinchang, J., Yarmahmoudi, A. "Optimization of Stirling Engine Heat Exchangers" Proc. of WSEAS Conf. Cantabria (Spain) Sept. 2008, p. 143-150 Available at: < http://www.wseas.us/e-library/conferences/2008/spain/selected/selected17.pdf > [accessed 15.1.2020]

[8] Sage Software for Engineering Modeling and Optimization. Available at: <https://www.sageofathens.com/> [accessed 15.1.2020]

[9] Ernst D. W., Shaltens, R. K., "Automotive Stirling Engine Development Project" Nasa report, Feb. 1997. Available at: <https://ntrs.nasa.gov/archive/nasa/casi.ntrs.nasa.gov/19970012689.pdf> [accessed 15.1.2020]

[10] Baumuller, A.; Borras, F.X.; Eskilson, P.; Nilsson, M.; Verner, A., "Upgrading of Stirling Engine Dynamic Seals-Swedish Development since 40 years". 17th Int. Stirling Engine Conf. (ISEC), 2016. Bilbao, Spain. Available at:
<https://www.researchgate.net/publication/323800615_Upgrading_of_Stirling_Engine_Dynamic_Seals_-_Swedish_Development_since_40_years> [accessed 15.1.2020]

[11] Wang, K., Sanders, S.R., Dubey, S., Choo, F.H "Stirling cycle engines for recovering low and moderate temperature heat: A review", Renewable and Sustainable Energy Reviews, 2016; 62: 89–108. Available at: <https://doi.org/10.1016/j.rser.2016.04.031> [accessed 15.1.2020]

[12] Organ, A. J., Rix, D.H., "Flow in the Stirling Regenerator Characterized in Terms of Complex Admittance Part 2: Experimental Investigation". Proc. of the Inst. of Mech. Engs., Part C: J of Mech Eng Sci, 1993; 207(2): 127-139.

[13] Cairelli, J. E., Kelm, G. G., Slaby, J. G., "Assessment of a 40-kilowatt Stirling engine for underground mining applications". Technical Report, NASA, June 1982. Available at: <https://ntrs.nasa.gov/search.jsp?R=19820022838> [accessed 15.1.2020]

[14] Flintney, R. Seal and Sealing Handbook. Fifth edition, Elsevier, 2007

[15] Fredy, C. "Modeling of the mechanical behavior of Polytetrafluoroethylene (PTFE) compounds during their compaction at room temperature", Doctorate thesis. Université Pierre et Marie Curie - Paris VI, 2015. Available at: <https://tel.archives-ouvertes.fr/tel-01336422/file/these_diffusion_3159619o.pdf> [accessed 15.1.2020]

[16] Technical data sheet Fluteck P7500 CA, PTFE carbon compound. Fluorseals Italy, 2015. Available at: <www.fluorseals.fi> [accessed 15.1.2020]

[17] How do Mises and Tresca Fit In. Available at:
<https://www.failurecriteria.com/misescriteriontr.html> [accessed 17.1.2020]